
Supplementary Materials

Graphene Bridge for Photocatalytic Hydrogen Evolution with Gold Nanocluster Co-Catalysts

Hanieh Mousavi ¹, Thomas D. Small ¹, Shailendra K. Sharma ², Vladimir B. Golovko ², Cameron J. Shearer ^{1,*} and Gregory F. Metha ^{1,*}

¹ Department of Chemistry, University of Adelaide, Adelaide SA 5005, Australia;

² The MacDiarmid Institute for Advanced Materials and Nanotechnology, School of Physical and Chemical Sciences, University of Canterbury, Christchurch 8140, New Zealand;

* Correspondence: cameron.shearer@adelaide.edu.au (C.J.S.); greg.metha@adelaide.edu.au (G.F.M.)

Contents

<u>1.</u>	<u>List of Figures</u>	3
<u>2.</u>	<u>Supplementary experimental details</u>	4
<u>2.1</u>	<u>Methodology optimisation of photocatalysts preparation</u>	4
<u>2.2.1</u>	<u>The effect of Au mass loading on HER activity of Au₁₀₁NC-AlSrTiO₃:rGO</u>	4
<u>2.2.2</u>	<u>The effect of heating in air and under vacuum on HER activity of Au₁₀₁NC-AlSrTiO₃:rGO</u>	4
<u>3.</u>	<u>Supplementary experimental results and discussion</u>	4
<u>3.1</u>	<u>Physical characterization</u>	4
<u>3.2</u>	<u>Photocatalytic hydrogen evolution activity</u>	7
<u>3.2.1</u>	<u>The effect of Au mass loading on HER activity of Au₁₀₁NC-AlSrTiO₃:rGO</u>	7
<u>3.2.2</u>	<u>The effect of heating in air and under vacuum on HER activity of Au₁₀₁NC-AlSrTiO₃:rGO</u>	8
<u>3.2.3</u>	<u>Appearance of Au₁₀₁NC-AlSrTiO₃:rGO and Au₁₀₁NC-rGO:AlSrTiO₃ before and after photocatalytic HER</u> ...	8
<u>4.</u>	<u>References</u>	10

1. List of Figures and Tables

Figure S1. The SEM image of AlSrTiO ₃	4
Figure S2. (a-b) HAADF-STEM images and (c) size distribution histogram of unsupported Au ₁₀₁ NC dropcast onto a TEM grid from methanol solution.	5
Figure S3. BF-STEM images of Au ₁₀₁ NC-AlSrTiO ₃ :rGO (a) before and (b) after HER and Au ₁₀₁ NC-rGO:AlSrTiO ₃ (c) before and (d) after HER. Au mass loading: 0.05 wt%. Annealing was performed at 210 °C in air for 15 min.	5
Figure S4. EDX spectra of a chosen spot on (a) rGO in Au ₁₀₁ NC-AlSrTiO ₃ :rGO and (b) AlSrTiO ₃ in Au ₁₀₁ NC-rGO:AlSrTiO ₃ . Annealing was performed at 210 °C in air for 15 min. The inserts are the HAADF-STEM images of the chosen area.	6
Figure S5. EDX spectra of a chosen spot on rGO in (a) Au ₁₀₁ NC-AlSrTiO ₃ :rGO-HER and (b) Au ₁₀₁ NC-rGO:AlSrTiO ₃ -HER. Annealing was performed at 210 °C in air for 15 min. The inserts are the HAADF-STEM images of the chosen area.	6
Figure S6. UV Vis DRS of Au ₁₀₁ NC-AlSrTiO ₃ :rGO and Au ₁₀₁ NC-rGO:AlSrTiO ₃ compared to AlSrTiO ₃ (a) before and (b) after HER. Annealing was performed in air at 210 °C for 15 min.	7
Figure S7. Sacrificial liquid phase H ₂ photocatalysis of Au ₁₀₁ NC-AlSrTiO ₃ :rGO (210 °C in air for 15 min) with Au mass loading of 0.05 and 1 wt%. (Conditions: 1:2 Methanol:Water, 365 nm at 83 mW/cm ² , 2 h reaction time).	8
Figure S8. Sacrificial liquid phase H ₂ photocatalysis of unannealed, annealed (air), and annealed (vacuum) Au ₁₀₁ NC-AlSrTiO ₃ :rGO. Au mass loading 1 wt%, 1:2 Methanol:Water, LED 365 nm at 83 mW/cm ² for 2 h. Annealing was performed at 210 °C for 15 min.	8
Figure S9. Photographs showing sample dispersions of (a) Au ₁₀₁ NC-AlSrTiO ₃ :rGO and (b) Au ₁₀₁ NC-rGO:AlSrTiO ₃ before (left images) and after (right images) photocatalytic HER. Au mass loading 0.05 wt%, 1:2 Methanol:Water, LED 365 nm at 83 mW/cm ² for 2h. Annealing was performed at 210 °C in air for 15 min.	9
Figure S10. Photographs showing dispersions of Au ₁₀₁ NCs (1 mg mL ⁻¹) in (a) 1:2 Methanol:Water and (b) Methanol.	10
Table S1. Average external quantum efficiencies (EQE)% for synthesized photocatalysts, assuming 2 electrons per H ₂ molecule produced.	

2. Supplementary experimental details

2.1 Methodology optimisation of photocatalysts preparation

2.2.1 The effect of Au mass loading on HER activity of Au₁₀₁NC-AlSrTiO₃:rGO

To make 10 mg Au₁₀₁NC-AlSrTiO₃:rGO with 0.05 and 1 wt% Au, 6.4 μ L and 128 μ L of an Au₁₀₁NC dispersion (1 mg mL⁻¹ ligated Au mass) were added dropwise to 10 mg of AlSrTiO₃ dispersed in 2 mL methanol in a porcelain evaporating dish and homogenised using bath sonication at RT until the solvent completely evaporated. The as-obtained Au₁₀₁NC-AlSrTiO₃ samples were dispersed and homogenised in 2 mL methanol via bath sonication (2 min). Then 16.6 μ L of the as-synthesized rGO dispersion was added dropwise to each dispersion with bath sonication at RT until the solvent completely evaporated. The as-obtained Au₁₀₁NC-AlSrTiO₃:rGO samples were annealed in a muffle furnace at 210 °C in air for 15 min.

2.2.2 The effect of heating in air and under vacuum on HER activity of Au₁₀₁NC-AlSrTiO₃:rGO

The as-obtained Au₁₀₁NC-AlSrTiO₃:rGO with 1 wt% of Au was placed in a porcelain evaporating dish was annealed in air in a muffle furnace and vacuum (< 0.01 bar) in a tube furnace (Across International, STF1200, quartz tube) at 210 °C for 15 min. This sample was compared with unannealed Au₁₀₁NC-AlSrTiO₃:rGO using photocatalysis.

3. Supplementary experimental results and discussion

3.1 Physical characterization

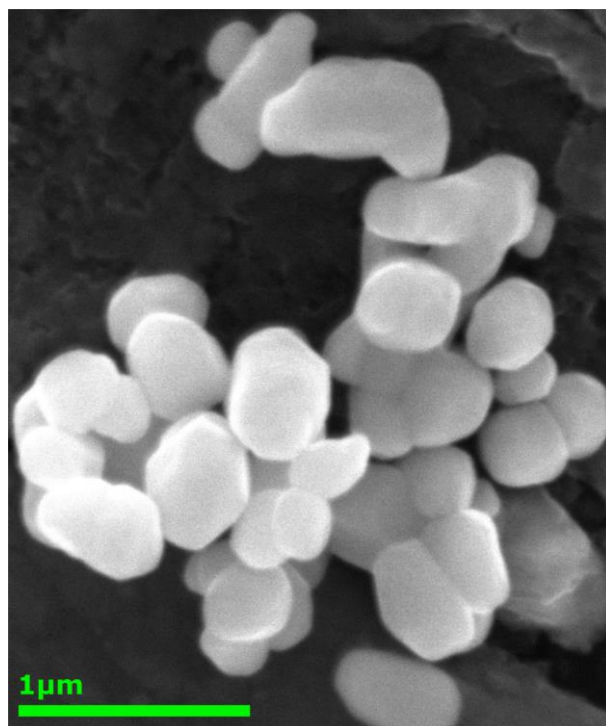


Figure S1. SEM image of AlSrTiO₃.

In order to determine if the size of the AuNCs changes during the formation of the photocatalyst, it is first required to benchmark the size of the as-prepared AuNCs. Figure S2(a-c) presents the high-resolution HAADF-STEM images and the measured cluster size histogram fitted to a log-normal distribution. The Au₁₀₁NCs have a mean diameter of 1.74 ± 0.29 nm and a mode of 1.52 nm. 3.9% of the clusters have diameters smaller than 1 nm and 25.6 % larger than 2 nm. In our previous publication which used a different batch of Au₁₀₁NC, we measured an average diameter of 1.3 ± 0.4 nm with 26.4% of particles less than 1 nm and 3.4 % greater than 2 nm [1].

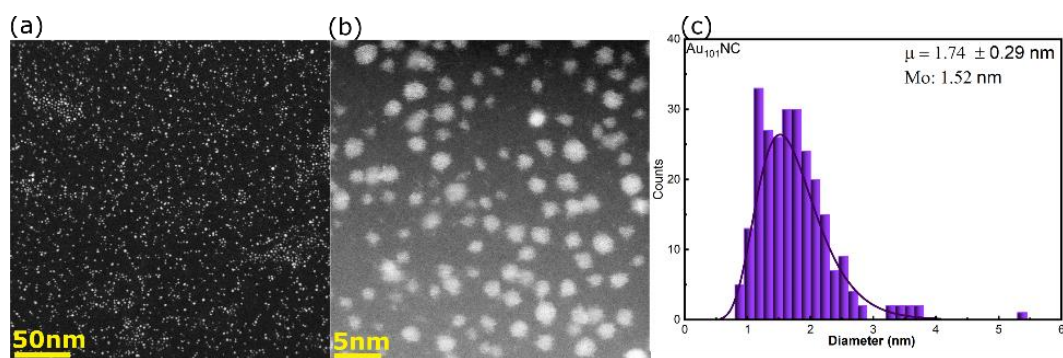


Figure S2. (a-b) HAADF-STEM images and (c) size distribution histogram of unsupported Au₁₀₁NC dropcast onto a TEM grid from methanol solution.

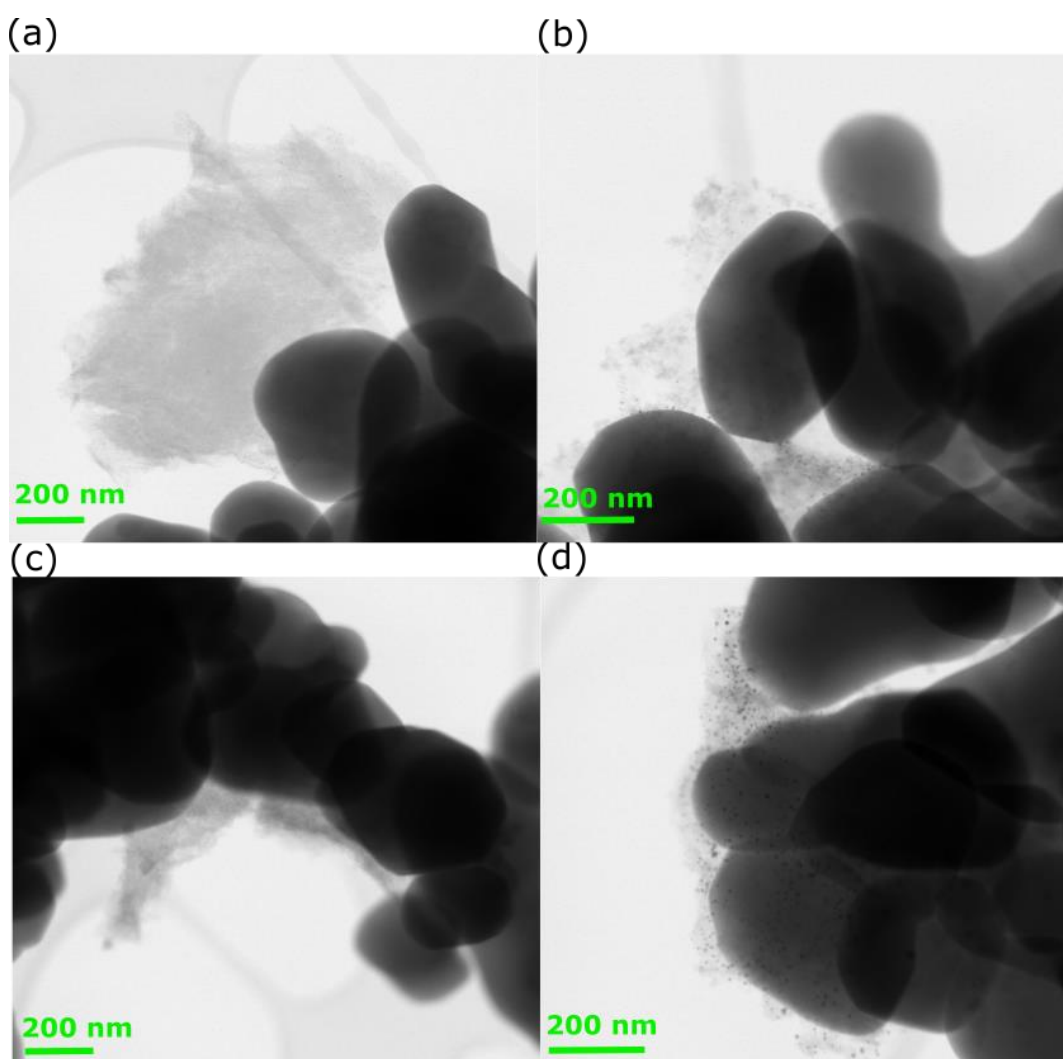


Figure S3. BF-STEM images of Au₁₀₁NC-AlSrTiO₃:rGO (a) before and (b) after HER and Au₁₀₁NC-rGO:AlSrTiO₃ (c) before and (d) after HER. Au mass loading: 0.05 wt%. Annealing was performed at 210 °C in air for 15 min.

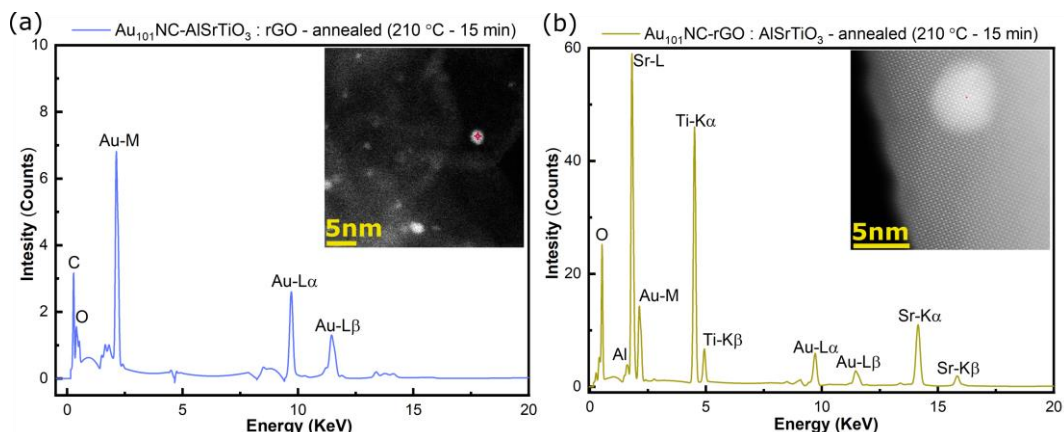


Figure S4. EDX spectra of the selected spot on (a) rGO in $\text{Au}_{101}\text{NC-AlSrTiO}_3:\text{rGO}$ and (b) AlSrTiO_3 in $\text{Au}_{101}\text{NC-rGO}:\text{AlSrTiO}_3$. Annealing was performed at 210°C in air for 15 min. The inserts are the HAADF-STEM images of the chosen area.

EDX spectra from a selected area of rGO from $\text{Au}_{101}\text{NC-AlSrTiO}_3:\text{rGO-HER}$ and $\text{Au}_{101}\text{NC-rGO}:\text{AlSrTiO}_3\text{-HER}$ samples is shown in Figure S5(a-b). Interestingly, in both samples, signal from SrTiO_3 is seen on rGO after, but not before, HER. Future work is required to find out how this occurs and its possible effect on photocatalytic activity.

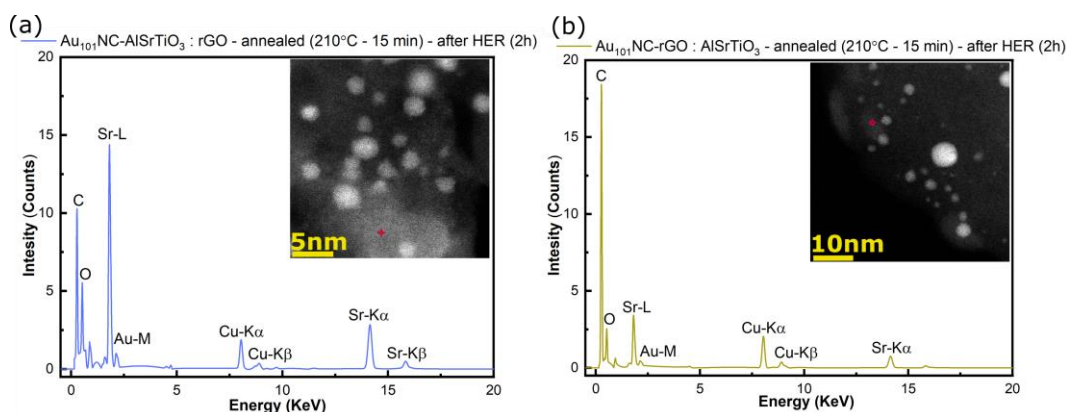


Figure S5. EDX spectra of a selected spot on rGO in (a) $\text{Au}_{101}\text{NC-AlSrTiO}_3:\text{rGO-HER}$ and (b) $\text{Au}_{101}\text{NC-rGO}:\text{AlSrTiO}_3\text{-HER}$. Annealing was performed at 210°C in air for 15 min. The inserts are the HAADF-STEM images of the chosen area.

UV-Vis DRS was used to measure the optical properties and agglomeration state of Au_{101}NC for the as-prepared $\text{Au}_{101}\text{NC-AlSrTiO}_3:\text{rGO}$ and $\text{Au}_{101}\text{NC-rGO}:\text{AlSrTiO}_3$ before and after photocatalysis and compared to AlSrTiO_3 (Figure S6(a-b)). In Figure S6(a), AlSrTiO_3 exhibits a typical absorption edge at 387 nm indicating a band gap of 3.2 eV. The bandgap of AlSrTiO_3 and the UV light absorption intensity are effectively identical upon addition of both rGO and Au_{101}NC onto AlSrTiO_3 , indicating that the electronic structure and optical properties of the AlSrTiO_3 are not altered. The slight absorption from 385 – 800 nm is due to the visible light absorbance of rGO [2]. The photocatalysis was performed at 365 nm (3.4 eV), where AlSrTiO_3 has strong absorbance and Au_{101}NC and rGO has negligible UV light absorbance. Additionally, no peak at ca. 520 nm due to Au surface plasmon resonance was observed, indicating that there is no agglomeration of Au_{101}NC deposited onto either rGO or AlSrTiO_3 . Likewise, evolving hydrogen under illumination did not cause agglomeration of the Au_{101}NC , as no peak at 520 nm was observed for samples that were measured after performing HER for two hours.

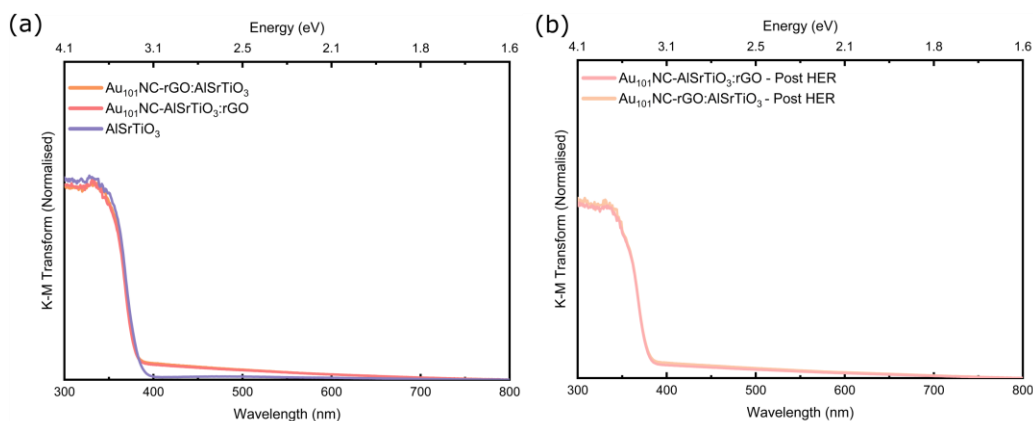


Figure S6. UV-Vis DRS of $\text{Au}_{101}\text{NC-AlSrTiO}_3\text{:rGO}$ and $\text{Au}_{101}\text{NC-rGO:AlSrTiO}_3$ compared to AlSrTiO_3 (a) before and (b) after HER. Annealing was performed in air at 210 °C for 15 min.

3.2 Photocatalytic hydrogen evolution activity

Table S1. Average external quantum efficiencies (EQE)% for synthesized photocatalysts, assuming 2 electrons per H_2 molecule produced.

Photocatalyst	Average H_2 EQE% (at 2 hours)
rGO	0.00046
AlSrTiO_3	0.00079
$\text{Au}_{101}\text{NC-rGO}$	0.00035
$\text{Au}_{101}\text{NC-rGO:AlSrTiO}_3$	0.04304
$\text{Au}_{101}\text{NC-AlSrTiO}_3$	0.00513
$\text{Au}_{101}\text{NC-AlSrTiO}_3\text{:rGO}$	0.04964
rGO-AlSrTiO_3	0.00507

3.2.1 The effect of Au mass loading on HER activity of $\text{Au}_{101}\text{NC-AlSrTiO}_3\text{:rGO}$

Figure S7 presents the effect of Au mass loading (0.05% and 1 wt%) on the photocatalytic HER activity in the $\text{Au}_{101}\text{NC-AlSrTiO}_3\text{:rGO}$ nanocomposite. Increasing the Au mass loading by 20 times results in a $\times 1.6$ increase in photocatalytic activity with the average H_2 production rate changing from 334 ± 24 to $539 \pm 14 \text{ nmol h}^{-1}$.

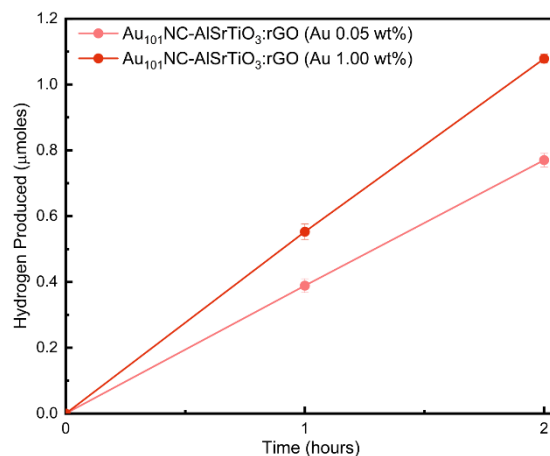


Figure S7. Sacrificial liquid phase H₂ photocatalysis of Au₁₀₁NC-AlSrTiO₃:rGO (210 °C in air for 15 min) with Au mass loading of 0.05 and 1 wt%. (Conditions: 1:2 Methanol:Water, 365 nm at 83 mW/cm², 2 h reaction time).

3.2.2 The effect of heating in air and under vacuum on HER activity of Au₁₀₁NC-AlSrTiO₃:rGO

To optimize the synthesis of photocatalysts, different annealing methods (air and vacuum) were applied. Figure S8 presents the effect of heating in air and under vacuum at 210 °C for 15 min on the photocatalytic HER activity of Au₁₀₁NC-AlSrTiO₃:rGO with 1% Au mass loading compared with unannealed samples. The photocatalytic activity was found to increase in the order; air annealing > vacuum annealing > not annealed, with average H₂ production rates of 1110, 510, and 320 nmol after 2h, respectively. Future work is required to find out the reasons for high HER activity of photocatalysts in air than vacuum.

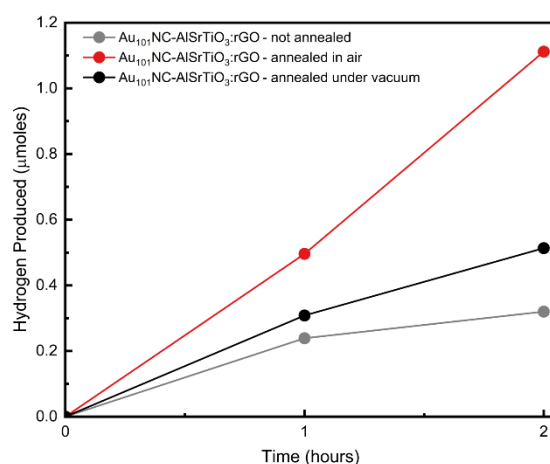


Figure S8. Sacrificial liquid phase H₂ photocatalysis of unannealed, annealed (air), and annealed (vacuum) Au₁₀₁NC-AlSrTiO₃:rGO. Au mass loading 1 wt%, 1:2 Methanol:Water, LED 365 nm at 83 mW/cm² for 2 h. Annealing was performed at 210 °C for 15 min.

3.2.3 Appearance of Au₁₀₁NC-AlSrTiO₃:rGO and Au₁₀₁NC-rGO:AlSrTiO₃ before and after photocatalytic HER

Figure S9(a-b) shows photographs of the AlSrTiO₃:rGO and Au₁₀₁NC-rGO:AlSrTiO₃ dispersion solutions used for photocatalytic HER. There is no observable change in the solution colour indicating the resistance of the as-prepared nanocomposites toward agglomeration (i.e. no presence of Au surface plasmon resonance), consistent with the DRS.

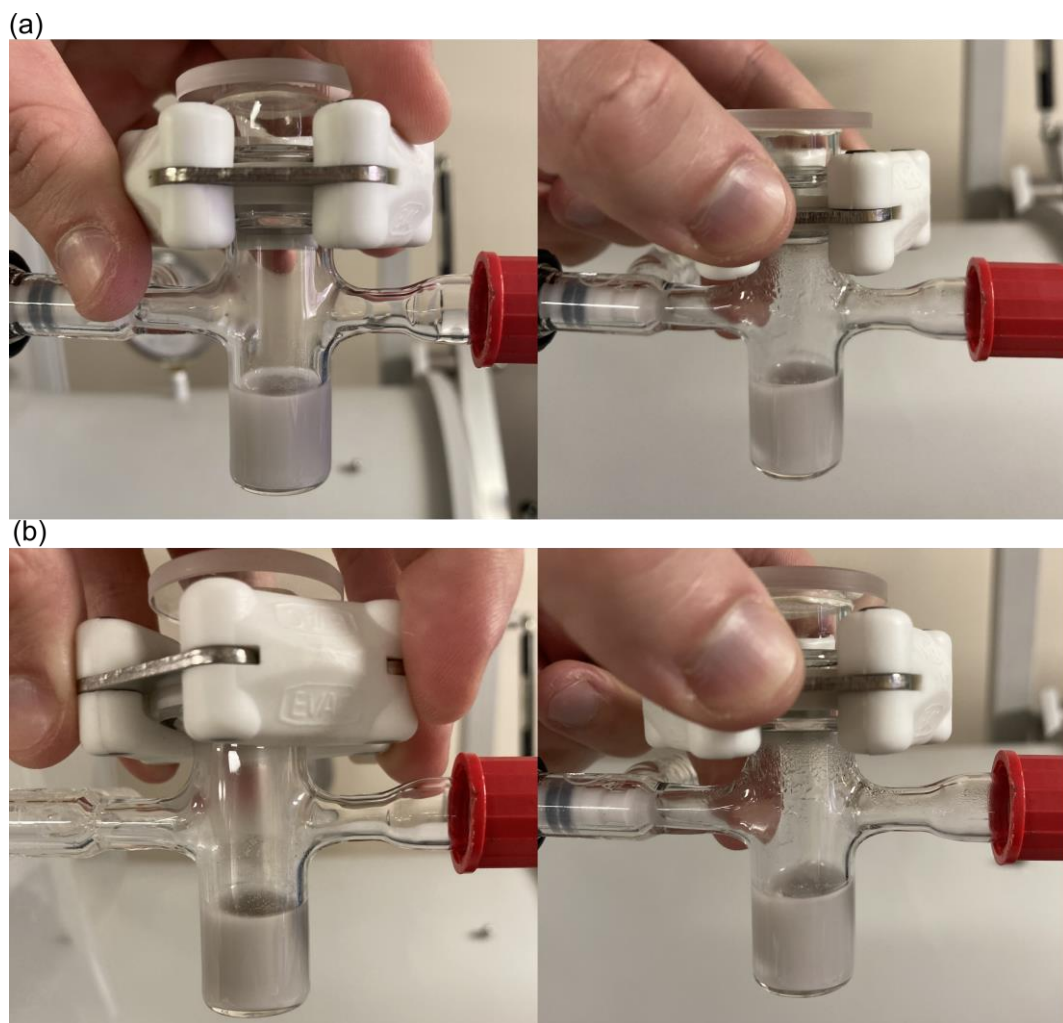


Figure S9. Photographs showing sample dispersions of the (a) $\text{Au}_{101}\text{NC-AlSrTiO}_3\text{:rGO}$ and (b) $\text{Au}_{101}\text{NC-rGO:AlSrTiO}_3$ samples before (left images) and after (right images) photocatalytic HER. Au mass loading 0.05 wt%, 1:2 Methanol:Water, LED 365 nm at 83 mW/cm² for 2h. Annealing was performed at 210 °C in air for 15 min.

Figure S10(a-b) shows the solubility of Au_{101}NC (1 mg mL⁻¹) in (a) 1:2 Methanol:Water and (b) Methanol. Au_{101}NC is highly soluble in methanol while it has very limited solubility in 1:2 Methanol:Water, indicating the adsorbed Au_{101}NC is unlikely to desorb from the surface of $\text{AlSrTiO}_3\text{/rGO}$ in 1:2 Methanol:Water during photocatalysis.

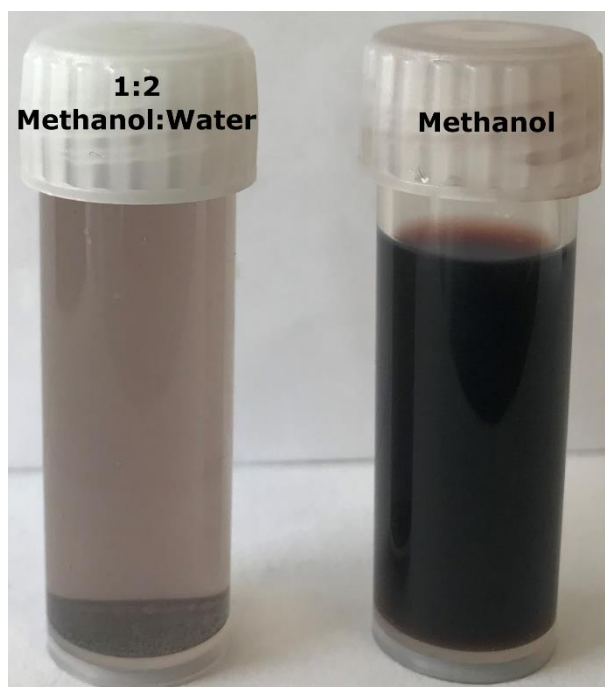


Figure S10. Photographs showing dispersions of Au₁₀₁NC (1 mg mL⁻¹) in (a) 1:2 Methanol:Water and (b) Methanol.

4. References

1. Mousavi, H.; Yin, Y.; Howard-Fabretto, L.; Sharma, S.K.; Golovko, V.; Andersson, G.G.; Shearer, C.J.; Metha, G.F. Au₁₀₁-rGO nanocomposite: Immobilization of phosphine-protected gold nanoclusters on reduced graphene oxide without aggregation. *Nanoscale Adv* **2021**, *3*, 1422-1430.
2. Albero, J.; Mateo, D.; García, H.J.M. Graphene-based materials as efficient photocatalysts for water splitting. *Molecules* **2019**, *24*, 906.